

INVESTIGATION OF CERIUM (III) ACTIVATED-CERIA NANOPARTICLES AS CORROSION INHIBITORS FOR CARBON STEEL

A. S. Nguyen^{1,*}, T. D. Nguyen¹, T. T. Thai¹, T. X. H. To^{1,2}

¹*Institute for Tropical Technology, VAST, 18 Hoang Quoc Viet, Hanoi, Vietnam*

²*Graduate University of Science and Technology, VAST, 18 Hoang Quoc Viet, Hanoi, Vietnam*

*Email: nason@itt.vast.vn

Received: 13 December 2017; Accepted for publication: 28 February 2018

Abstract. The present work investigated the corrosion protection performance of Ce(III) activated-cerium(IV) oxide nanoparticles for carbon steel in a NaCl solution. Ceria nanoparticles were synthesized by homogeneous precipitation in ethanol/water mixed solvent. The obtained CeO₂ nanoparticles were characterized by X-ray diffraction (XRD) and transmission electron microscope (TEM). The corrosion inhibition action of the activated nanoparticles by cerium(III) ions on carbon steel in NaCl solution was evaluated by electrochemical measurements (electrochemical impedance spectroscopy (EIS) and potentiodynamic polarization). Then, the effect of cerium salt activated-CeO₂ on the protection properties of poly-vinyl-butyril (PVB) coating deposited onto carbon steel plate was studied by salt spray test. The obtained results showed that the salt activated-nanoparticles are anodic corrosion inhibitors. The presence of Ce(III) activated CeO₂ in the coating improved the barrier properties and corrosion protection performance of the PVB coating. No swellings of coating were observed after 48 hours of exposure in salt spray chamber.

Keywords: corrosion, CeO₂, activated nanoparticles, EIS, salt spray test.

Classification numbers: 2.5.1, 2.5.3.

1. INTRODUCTION

Chromium hexavalent (Cr(VI)) compounds were well-known to have excellent corrosion protection that make them become standard corrosion inhibitors in industry painting [1-3]. However, the Cr(VI) species presented a very high toxicity and a bad environmental impact. For this reason, since the beginning of the 1990s, the chromates have imposed restrictions on their use in industrial applications and particularly in organic coatings [4].

During the last decades, several works were devoted to developing “green” alternative systems containing environmentally friendly inhibitors [5-7]. Among the novel tested compounds (Ce³⁺, Y³⁺, La³⁺...), the lanthanides ions became a potential candidate for substitution of the chromates due to their low toxicity [8] and their good anti-corrosion properties [9, 10].

Moreover, these compounds were economically competitive products, in particular cerium compounds can easily be found in nature. Many research had been undertaken to study the anti-corrosion efficiency of cerium salts for a number of metals and alloys, such as: aluminum, zinc, tin, steel, hot dip galvanized steel and their alloys, etc. [11-15]. The corrosion behavior of cerium salt was reported by Hayes et al. [16] and Yu et al. [17]. It was reported that the insoluble cerium compounds ($\text{Ce}(\text{OH})_4$ and CeO_2) were formed at the cathodic sites due to the production of OH^- ions. These elements were precipitated on the surface of metal that inhibited the corrosion phenomenon. However, when the cerium salts were incorporated into organic coatings as corrosion inhibitor, the barrier properties of the coating would usually decrease due to leaching process during exposure time. On the other hand, the usage of cerium(IV) oxide nanoparticles directly as inhibitor source was found [18-20]. These works demonstrated that the presence of nano- CeO_2 in sol-gel coatings increased the barrier performances and reduced the corrosion rate (about 1000 times compared to uncoated alloy). For enhancing the corrosion protection properties of the coatings, Montermor et al. [21] and Zand et al. [22] inserted the cerium salt activated nano- CeO_2 into silane coatings. The authors reported that the activation of the nanoparticles with Ce(III) ions enhanced both barrier and corrosion inhibition properties of silane film deposited onto galvanized steel.

Although there were a few works in literature that proved the corrosion performance of cerium ion activated ceria nanoparticles, the corrosion inhibition process of this compound on carbon steel in an aerated environment was still unclear. Thus, the aim of this work is to evaluate the corrosion inhibition effect of Ce(III) activated CeO_2 ($\text{Ce}^{3+}@\text{CeO}_2$) nanoparticle by comparison to cerium salt and cerium(IV) oxide for carbon steel substrate. The corrosion inhibition efficiency of Ce(III) activated nano- CeO_2 was investigated by electrochemical impedance spectroscopy (EIS) and potentiodynamic polarization curves. The corrosion protection performance of PVB coating containing Ce(III) activated nano- CeO_2 was evaluated by salt spray test.

2. MATERIALS AND METHODS

2.1. Materials and samples preparation

$\text{Ce}(\text{NO}_3)_3 \cdot 6\text{H}_2\text{O}$ and ammonia were purchased from Merck (Germany). poly-vinyl-butyril (PVB) was purchased from Sekisui (Japan).

Cerium(IV) oxide nanoparticles were prepared via homogeneous precipitation reported elsewhere [23]. Briefly, in this method, cerium(III) nitrate was dissolved in an ethanol/water (50:50) solvent. Then, 10 mL of 25 % ammonia was added slowly drop-wise into this solution. The reaction was taken place at 60 °C during 2 hours under stirring. The precipitation was finally collected by centrifugation, washed with distilled water until neutral pH, and dried at 70 °C overnight.

The obtained CeO_2 nanoparticles were activated with cerium(III) ions under ultrasonic condition. Due to present a fluorite structure, these nanoparticles easily form oxygen vacancies, that yield reactive sites. Thus, they could readily incorporate Ce^{3+} ions by forming charge-compensating defects on the oxygen sublattice [24, 25].

The metallic substrate was used in this work consisted of carbon steel XC35 rod (1 cm² cross-section) and plates (150 × 100 × 2 mm). Its chemical composition was C = 0.35 wt%, Mn = 0.65 wt%, Si = 0.25 wt%, P = 0.035 wt%, S = 0.035 wt% and Fe = balance. To evaluate the inhibitive efficiency in an aerated solution, the used carbon steel rod was covered by a heat-

shrinkable sheath (left only the tip of the cylinder in contact with the solution). The specimens were ground with SiC papers down to grade of 1200, washed with ethanol, and dried in warm air.

For the coatings samples, the metallic plates were ground with abrasive papers (400 grades) and cleaned with ethanol. Then, the poly-vinyl-butyril (PVB) coatings containing Ce(NO₃)₃ or CeO₂ or Ce³⁺@CeO₂ were deposited onto these plates by spin-coating method. In another experiment, coatings without inhibitors were also prepared. The amount of Ce(III) used in Ce(NO₃)₃ incorporated into coatings was at the same concentration as Ce(IV) used in CeO₂ for ensuring comparative results between these inhibitors. The thickness of coating obtained after 24 hours at room temperature was about 10 ± 1 μm (measured by MiniTest 600 Erichsen digital meter).

2.2. Analytical methods

The crystalline structure of as-prepared CeO₂ was characterized by X-ray diffraction (XRD, D8 Advance Bruker) with monochromated Cu K α radiation ($\lambda = 1.54 \text{ \AA}$). The powder was analyzed at the 2θ range from 20 to 80°. Transmission Electron Microscope (TEM) observation was done using a JEM-T8 at 80 kV.

Electrochemical measurements (EIS and potentiodynamic polarization) were carried out to study the corrosion performance of Ce(III) ions, CeO₂ nanoparticles and Ce³⁺@CeO₂ in a 0.1 M NaCl solution using Autolab PGSTAT30. A classical three-electrode system was used, in which a XC35 rod was rotating disk electrode (500 rpm) as working electrode, a saturated calomel (SCE) and platinum grid were used as reference and counter electrodes, respectively. The impedance diagrams were taken at the open circuit potential (OCP), under potentiostatic condition, over a frequency range from 100 kHz to 10 mHz with an amplitude of 10 mV. After 20 hours of exposure in 0.1 M NaCl solution containing the tested inhibitors, the anodic and cathodic polarization curves were recorded at a scan rate of 1 mV s⁻¹. For each experiment, measurements were performed three times.

Salt spray test was realized by Q-FOGCCT-600 chamber according to ASTM B117. A 5% NaCl solution was sprayed on the samples during the test at 35 °C. Before exposure in the chamber, the scratches were manually created on the surface of each specimen by a cutting knife according to ISO 17872. The scratch was approximately 110 μm width. The tested plates were supported 20 degrees from the vertical and preferably parallel to the principal direction and without any contact each other in chamber. The samples were observed at the end of the test (48 hours).

3. RESULTS AND DISCUSSION

3.1. Characterization of synthesized CeO₂ nanoparticles

The XRD pattern of obtained CeO₂ nanoparticles is shown in Fig. 1. The characteristic peaks locate at $2\theta = 28.6, 33.1, 47.4, 56.3, 59.2, 59.5, 76.6$ and 79.0 degrees corresponding to (111), (200), (220), (311), (222), (400), (331) and (420) lattice planes of CeO₂, respectively [23,26]. By using the standard data JCPDS 34-0394, it can be concluded that the obtained peaks in XRD pattern presented planes of a cubic fluorite structure (space group: Fm $\bar{3}$ m) of CeO₂. From XRD pattern, the crystalline size of CeO₂ can be estimated by using Scherrer equation at characteristic peak (111):

$$d = \frac{0.9\lambda}{FWHM \cos\theta} \quad (1)$$

where λ , FWHM and θ are the wavelength of X-rays, the full width at half maximum in radians and the diffraction angle for the (111) plan, respectively. The crystalline size of synthesized nano-CeO₂ was calculated about 9.6 nm.

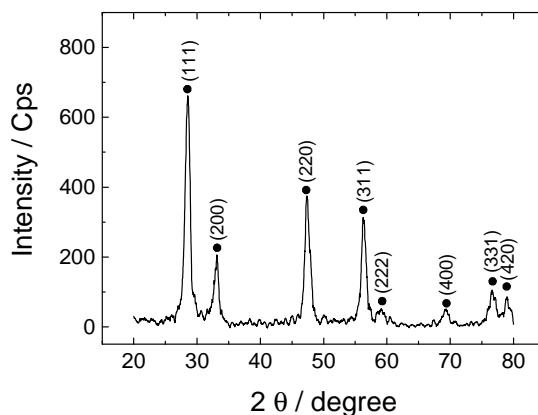


Figure 1. X-ray diffraction spectra of synthesized nano-CeO₂.

The TEM image of obtained nanoparticles in ethanol is presented in Fig. 2. It can be observed that the shape of as-prepared CeO₂ is hexagonal and the average particle size is about 11 nm. The result confirms the size value calculated from the XRD pattern and the particle is a single crystal.

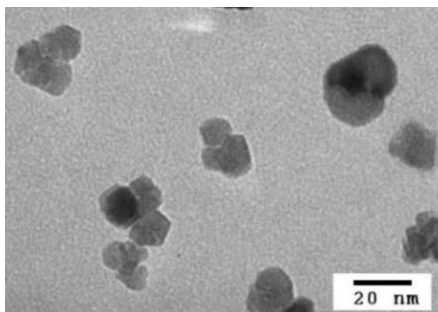


Figure 2. TEM photograph of synthesized CeO₂ nanoparticles.

3.2. Corrosion inhibition test

The obtained CeO₂ nanoparticles, Ce(NO₃)₃ and Ce³⁺@CeO₂ were dispersed separately in a 0.1 M NaCl solution under ultrasonic condition for 5 min. The obtained polarization curves after 20 h of immersion in these solutions are presented in Fig. 3. In the presence of CeO₂ in the 0.1 M NaCl solution, it had a very slightly different compared to the curve obtained in the blank solution. The polarization curves measured in the solution containing Ce(NO₃)₃ showed a decrease of both anodic and cathodic current densities and the corrosion potential toward more positive value (-0.59 V compared to -0.63 V for blank solution). It indicated that the cerium salt is a mixed inhibitor acting both on the anodic and cathodic processes. The corrosion potential that measured in the solution containing Ce³⁺@CeO₂ nanoparticles is the most positive ($E_{\text{corr}} = -$

0.56 V). However, the obtained polarization curves presented higher anodic and cathodic current densities compared to that in the case of Ce(NO₃)₃ presence, it means that Ce³⁺@CeO₂ is a less inhibitor compared to Ce(NO₃)₃ salt for carbon steel.

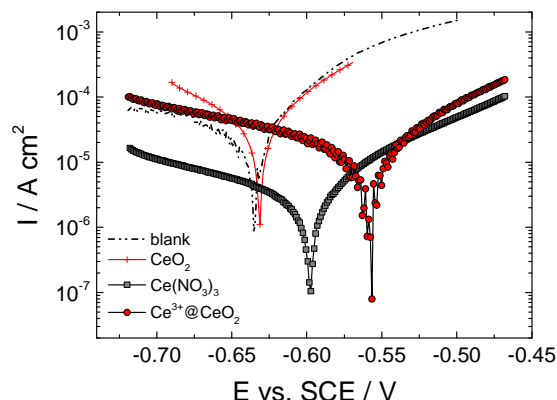


Figure 3. Polarization curves for the carbon steel after 20 h of exposure in a 0.1 M NaCl solution containing different inhibitors (indicated on the figure).

Figure 4 shows impedance diagrams (Bode coordinates) obtained for the carbon steel rotating electrode in these solutions after 20 hours of immersion. For the solution containing CeO₂ nanoparticles, the impedance modulus and phase angle presented a little difference compared to the curves obtained for the 0.1 M NaCl solution without inhibitors. It means that, at low concentration, inhibitive effect of CeO₂ nanoparticles is negligible. When these nanoparticles were activated by cerium(III) ions, the impedance module value increased about $6 \times 10^3 \Omega \text{ cm}^2$ and the phase angle at 1 Hz is about 45°. It can be explained that after being activated, Ce³⁺@CeO₂ nanoparticles are better dispersed in the solution due to increase of average surface charge (shifted to a more positive, the results of zeta potential were not reported here) and with the presence of Ce³⁺ on the surface of nanoparticles, they formed a protective film on the working electrode. However, the impedance value of this film is lower than that of which obtained in the solution containing Ce(NO₃)₃ salt.

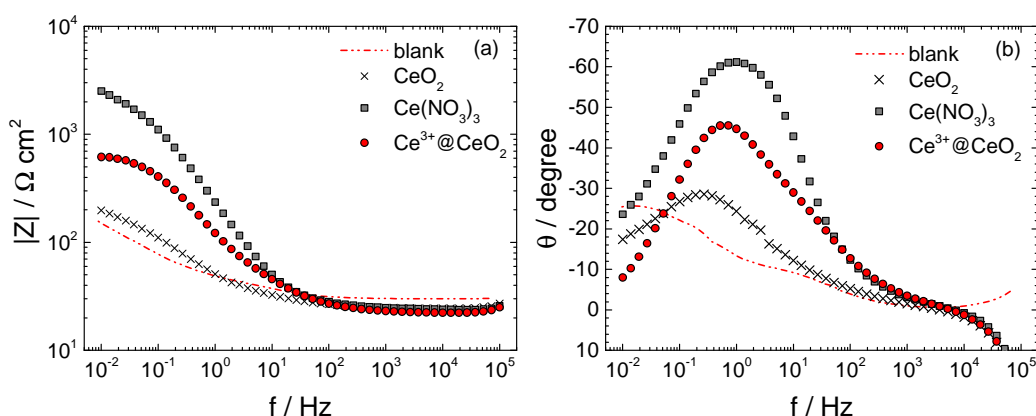


Figure 4. Impedance response in Bode for the carbon steel rod obtained after 20 hours of immersion in a 0.1 M NaCl solution containing different inhibitors (indicated on the figure).

Additionally, the inhibitor efficiency (IE) can be evaluated by using the value of the polarization resistance obtained from impedance diagram according equation:

where R_p and R_{p0} are the polarization resistances values obtained in the solution containing inhibitors and in the blank solution (determined by extrapolation at the low frequency of 10 mHz from the impedance diagrams), respectively. The measured values are reported in Table 1. It shows that the inhibitor efficiency of Ce(III) salt is higher than that of $Ce^{3+}@CeO_2$. This is in line with the conclusion of polarization study above.

Table 1. Parameters extracted from the impedance diagrams at the frequency of 10 mHz.

Compound	($\Omega\text{ cm}^2$)	Inhibitor efficiency (%)
Blank	275	-
CeO_2	300	8
$Ce(NO_3)_3$	2700	90
$Ce^{3+}@CeO_2$	700	61

The salt spray test was carried out to accelerated test for the corrosion protection of the coatings containing the inhibitors as CeO_2 or $Ce(NO_3)_3$ or $Ce^{3+}@CeO_2$ (Fig. 5). Around the scratches, the delamination zone observed for PVB coatings without doped inhibitors is much larger than that for the rest of samples. The PVB coating containing $Ce^{3+}@CeO_2$ shows less corrosion products in the scratch than the others. Some corrosion points can be seen on the PVB and PVB- CeO_2 coatings. It reports that there was not any swelling detected around the scratch of PVB- $Ce^{3+}@CeO_2$ coating while it can be clearly observed on surface of PVB- $Ce(NO_3)_3$ coating.

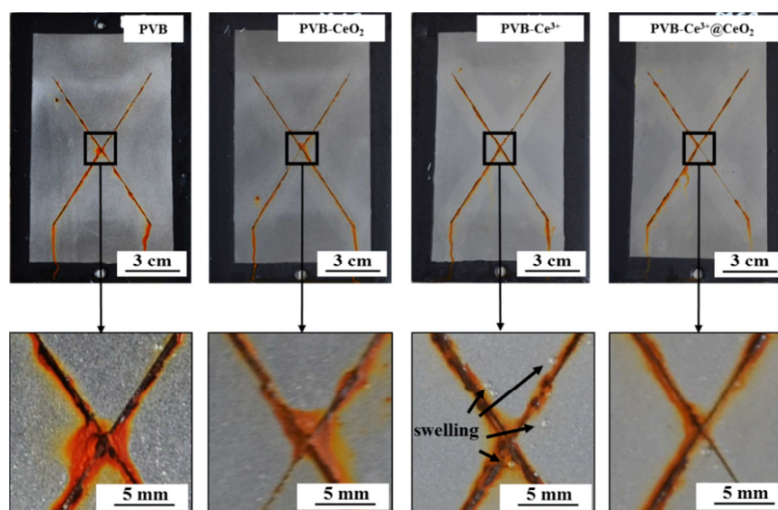


Figure 5. Salt spray photographs of PVB coatings doped the different inhibitors on carbon steel plate after 48 hours of exposure.

This phenomenon was due to the leaching of cerium nitrate (high solubility) during the test, and the salt solution was replaced into the space of $Ce(NO_3)_3$ in the coating system. The results

demonstrate that the Ce³⁺@CeO₂ nanoparticles have better corrosion protection effect compared with cerium(III) salt for the organic coatings. The presence of this compound improves both barrier and corrosion protection properties of the organic coatings, in particular poly-vinyl-butyril model coating.

4. CONCLUSIONS

This work focused to investigate the corrosion protection performance of cerium salt activated-cerium(IV) oxide nanoparticles in NaCl solution and in organic coating by comparative study with CeO₂ nanoparticles and Ce(NO₃)₃. The size of CeO₂ nanoparticles obtained about 11 nm by homogeneous precipitation technique. In a 0.1 M NaCl solution, the cerium salt and cerium(III) ion activated-nanoparticles presented the protective films on the working electrode. The inhibition efficiency of Ce(NO₃)₃ was higher than that of Ce³⁺@CeO₂. However, the presence of Ce³⁺@CeO₂ nanoparticles in poly-vinyl-butyril coating showed a better barrier and anticorrosion properties in comparison to the incorporation of Ce(NO₃)₃ in the same type coating. Due to a high solubility of cerium(III) nitrate, the coating containing Ce(NO₃)₃ presented a lot of swelling points around the scratch which could not be seen in the case of Ce(III) ion activated CeO₂ nanoparticles doped PVB coating after spray test.

Acknowledgements. The authors gratefully acknowledge the financial support of Vietnam Academy of Science and Technology.

REFERENCES

1. Zin I. M., Howard R. L., Badger S. J., Scantlebury J. D., Lyon S. B. - The mode of action of chromate inhibitor in epoxy primer on galvanized steel, *Prog. Org. Coat.* **33** (1998) 203-210.
2. Corfias C., Pebere N., Lacabanne C. - Characterization of a thin protective coatings on galvanized steel by electrochemical impedance spectroscopy and a thermostimulated current method, *Corros. Sci.* **41** (1999) 1539-1555.
3. Nguyen A. S., Pebere N. - A local electrochemical impedance study of the self-healing properties of waterborne coatings on 2024 aluminium alloy, *Electrochim. Acta* **222** (2016) 1806-1817.
4. Regulation (EC) 1907/2006 of the European Parliament and of the Council on the Registration, Evaluation, Authorisation and Restriction of Chemicals (REACH).
5. To T. X. H., Trinh A. T., Nguyen T. D., Pebere N., Olivier M. G. - Layered double hydroxides as containers of inhibitors in organic coatings for corrosion protection of carbon steel, *Prog. Org. Coat.* **74** (2012) 343-348.
6. Kartsonakis I. A., Athanasopoulou E., Snihirowa D., Martins B., Koklioti M. A., Montemor M. F., Kordas G., Charitidis C. A. - Multifunctional epoxy coatings combining a mixture of traps and inhibitor loaded nanocontainers for corrosion protection of AA2024-T3, *Corros. Sci.* **85** (2014) 147-159.
7. Cao Y., Dong S., Zheng D., Wang J., Zhang X., Du R., Song G., Lin C. - Multifunctional inhibition based on layered double hydroxides to comprehensively control corrosion of carbon steel in concrete, *Corros. Sci.* **126** (2017) 166-179.

8. Mishra A. K., Balasubramaniam R., Tiwari S. - Corrosion inhibition of 6061-SiC by rare earth chlorides, *Anti-Corros. Method M.* **54** (2007) 37-46.
9. Khaled K. F. - Electrochemical evaluation of environmentally friendly cerium salt as corrosion inhibitor for steel in 3.5 % NaCl, *Int. J. Electrochem. Sci.* **8** (2013) 3974-3987.
10. Wang X., Gao Y., Li Y., Yang T. - Effect of yttrium on the corrosion behavior of 09CrCuSb alloy in NaCl solution, *Corros. Sci.* **87** (2014) 211-217.
11. Druart M-E., Recloux I., Thai T.T., Ershov S., Snyders R., Olivier M-G. - Impact of the addition of cerium salts (Ce(III) and Ce(IV)) on formation and ageing of a silica sol-gel layer, *Surf. Coat. Technol.* **304** (2016) 40-50.
12. Aramaki K. - Treatment of zinc surface with cerium(III) nitrate to prevent zinc corrosion in aerated 0.5 M NaCl, *Corros. Sci.* **43** (2001) 2201-2215.
13. Arenas M. A., Damborenea J. de- Protection of Zn-Ti-Cu alloy by cerium trichloride as corrosion inhibitor, *Surf. Coat. Technol.*, **200** (2005) 2085-2091.
14. Motte C., Maury N., Olivier M-G., Petitjean J-P., Willem J-F. - Cerium treatments for temporary protection of electroplated steel, *Surf. Coat. Technol.* **200** (2005) 2366-2375.
15. Zand R. Z., Verbeken K., Adriaens A. - Influence of the cerium concentration on the corrosion performance of Ce-doped silica hybrid coatings on hot dip galvanized steel substrates, *Int. J. Electrochem. Sci.* **8** (2013) 548-563.
16. Hayes S. A., Yu P., O'Keefe T. J., O'Keefe M. J., Stoffer J. O. - The phase stability of cerium species in aqueous systems - I. E-pH diagram for the Ce-HClO₄-H₂O system, *J. Electrochem. Soc.*, **149** (2002) C623-C630.
17. Yu P., Hayes S. A., O'Keefe T. J., O'Keefe M. J., Stoffer J. O. - The phase stability of cerium species in aqueous systems - II. The Ce(III/IV)-H₂O-H₂O₂/O₂ systems. Equilibrium considerations and Pourbaix diagram calculations, *J. Electrochem. Soc.* **153** (2006) C74-C79.
18. Schem M., Schmidt T., Gerwann J., Wittmar M., Veith M., Thompson G. E., Molchan I. S., Hashimoto T., Skeldon P., Phani A.R., Santucci S., Zheludkevich M.L. - CeO₂-filled sol-gel coatings for corrosion protection of AA2024-T3 aluminium alloy, *Corros. Sci.* **51** (2009) 2304-2315.
19. Ershad-Langroudi A., Rahimi A. - Effect of ceria and zirconia nanoparticles on corrosion protection and viscoelastic behavior of hybrid coatings, *Iran. Polym. J.* **23** (2014) 267-276.
20. Fedel M., Ahniyaz A., Ecco L. G., Deflorian F. - Electrochemical investigation of the inhibition effect of CeO₂ nanoparticles on the corrosion of mild steel, *Electrochim. Acta* **131** (2014) 71-78.
21. Montemor M. F., Ferreira M. G. S. - Cerium salt activated nanoparticles as fillers for silane films: evaluation of the corrosion inhibition performance on galvanized steel substrates, *Electrochim. Acta* **52** (2007) 6976-6987.
22. Zand R. Z., Verbeken K., Adriaens A. - Evaluation of the corrosion inhibition performance of silane coatings filled with cerium salt-activated nanoparticles on hot-dip galvanized steel substrat, *Int. J. Electrochem. Sci.* **8** (2013) 4924-4940.

23. Chen H. I., Chang H. Y. - Homogeneous precipitation of cerium dioxide nanoparticles in alcohol/water mixed solvents, *Colloids Surf. A: Physicochem. Eng. Aspects* **242** (2004) 61-69.
24. Cabot B., Foissy A. - Reversal of the surface charge of a mineral powder: application to electrophoretic deposition of silica for anticorrosion coatings, *J. Mater. Sci.* **33** (1998) 3945-3952.
25. Li R., Yabe S., Yamashita M., Momose S., Yoshida S., Yin S., Sata T. - Synthesis and UV-shielding properties of ZnO- and CaO-doped CeO₂ via soft solution chemical process, *Solid State Ionics* **151** (2002) 235-241.
26. Pan C., Zhang D., Shi L. - CTAB assisted hydrothermal synthesis, controlled conversion and CO oxidation properties of CeO₂ nanoplates, nanotubes, and nanorods, *J. Solid State Chem.* **181** (2008) 1298-1306.